Effects of focused ion beam induced damage on the plasticity of micropillars

Jaafar A. El-Awady,[1,*] Christopher Woodward,[1] Dennis M. Dimiduk,[1] and Nasr M. Ghoniem[2]

[1]*Air Force Research Laboratory, Materials and Manufacturing Directorate, AFRL/RXLM Wright-Patterson AFB, Ohio 45433-7817, USA*
[2]*Mechanical and Aerospace Department, University of California, Los Angeles, California 90095-1597, USA*

The hardening effects of focused ion beam (FIB) induced damage produced during the fabrication of micropillars are examined by introducing a surface layer of nanosized obstacles into a dislocation dynamics simulation. The influence of the depth and strength of the obstacles as a function of pillar diameter is assessed parametrically. We show that for a selected set of sample sizes between 0.5 and 1.0 μm, the flow strength can increase by 10–20 %, for an obstacle strength of 750 MPa, and damage depth of 100 nm. On the other hand, for sizes larger and smaller than this range, the effect of damage is negligible. Results show that the obstacles formed during the FIB milling may be expected to alter the microstructure of micropillars, however, they have a negligible effect on the observed size-strength scaling laws.

Focused ion beam (FIB) methods are site specific sample preparation techniques, that have been widely used for a couple of decades in semiconductor,[1,2] material science,[3–9] biology,[10,11] geoscience,[12] and many other disciplines. In FIB techniques, the shape of the target material is manipulated by bombarding the surface of the target by gallium accelerated heavy ions.

One possible draw back of the FIB process, is that gallium ions can critically alter the defect state of the target material. This could have an impact on samples with a large surface-to-volume ratio. The FIB induced damage observed in many conventional alloys, can be present in the form of an amorphous layer,[13,14] dislocation networks,[15,16] vacancy clusters in the form of staking fault tetrahedra,[17] interstitial loops, decoration of dislocations with Ga, as well as Ga precipitates.[15,16] Moreover, the depth and concentration of the FIB induced damage is dependent on the target material, ion acceleration energy, ion dose, and the ion incident angle.[14,18–20]

In a recent application of the FIB technique, Uchic *et al.* introduced a new experimental technique to quantify plasticity size dependency.[21] Via this technique, micropillars were milled from a bulk crystal using a FIB, then a uniform compression load was imposed on the top of the micropillar using a nanoindentor with a flat ended diamond tip. These experiments produced an unexpected dependence of strength and ductility on crystal size. This sparked a wide interest in the problem of plasticity size dependency in many conventional alloys.[3–9] From these results, it was suggested that the observed size effects are controlled mainly by the size distribution of the underlying sources and dislocation microstructure.[22]

Since these micropillars have a large surface-to-volume ratio, the effect of the FIB induced damage may critically alter the mechanical properties of these pillars. To investigate this, Kiener *et al.*,[4] investigated the damaged surface due to Ga ion bombardment during FIB milling of Cu micropillars. They reported a substantial depth of Ga implantation up to 50 μm. They also performed basic theoretical analysis to estimate the influence of a precipitation hardened damage layer. It was finally concluded that FIB damage limits the

applicability of microcompression tests, and that its effect may be proportional to the inverse of the micropillar size. In addition, Shim *et al.*[9] have shown that compressed Mo-alloy pillars in the as-grown condition, behave like dislocation free crystals, and yield at near-theoretical strength. On the other hand, micropillars that were FIB milled before compression, yielded at a much lower strength. These studies suggest that the FIB altered microstructure could play a significant role in the micropillar plasticity.

On the other hand, Shan *et al.*[6] performed *in situ* TEM compression experiments on Ni single-crystal micropillars. They observed that, for micropillars having sizes below 0.16 μm, the high density of initial defects produced by FIB milling were completely driven out of the crystal by the compression loading. The near-theoretical flow strength computed for these micropillars was observed to coincide with the elastic behavior of source-free mechanically annealed pillars. This suggests that, in contradictory to the theoretical estimates of Kiener *et al.*,[4] the precipitation hardened damage layer has a minimal effect at such very small scales. These experimental studies, as well as studies performed on Au micropillars,[5] suggest that the effects of the FIB milling is negligible if the original crystal has some initial dislocation structure before milling.

To study the size effects observed in micropillar compression experiments, a number of three-dimensional (3D) dislocation dynamics (DD) simulations were recently performed. These simulations led to discovery of key mechanisms that appear to govern the experimentally observed size effects.[23–25] Although, the results of such simulations are in general agreement with several experimental observations, all such DD simulations failed to address the effects that may arise due to the FIB induced damaged.

To address this, we used 3D DD simulations to investigate the effects of FIB induced damage on the observed micropillar strength size dependence. The computational method adopted here is that developed in.[26] In this formulation, the boundary element method is coupled with the 3D parametric dislocation dynamics formulation to incorporate the influence of interfaces on dislocation motion and to describe microscopic plastic flow in finite volumes. The simulations

mimic the compression experiments of Dimiduk *et al.*,[3] for compression of FCC single-crystal micropillars. The simulated micropillars are oriented in the [001] direction, have a fixed aspect ratio of 3:1, and the pillar diameters are in the range of $D=0.25-5.0$ μm. The initial dislocation density in all simulations ranges from $\rho=1\times10^{12}$ to 15×10^{12} m^{-2}, which is equivalent to those reported from experiments.[3,5] A compressive stress is applied to the top surface of the cylinder, while the bottom surface is kept fixed. Mimicking the loading technique of the experiments, a mixture of a constant strain rate loading, and a constant stress loading is applied. At any given time step, if the calculated plastic strain rate is smaller than the applied strain rate, $\dot{\varepsilon}_p<\dot{\varepsilon}$, the applied stress is increased to obey $\dot{\sigma}=E(\dot{\varepsilon}-\dot{\varepsilon}_p)$. On the other hand, if the computed plastic strain rate is greater than the applied strain rate, $\dot{\varepsilon}_p>\dot{\varepsilon}$, the applied stress is held constant, $\dot{\sigma}=0$. Once this condition is satisfied, the stress is kept constant until the total displacement becomes grater than the applied strain rate multiplied by the total elapsed time, $(\varepsilon_e+\varepsilon_p)<\dot{\varepsilon}\Delta t$. Finally, the applied strain rate in all simulations is $\dot{\varepsilon}=200$ s^{-1}, and the material properties chosen here are those of Ni.

Out of all forms of FIB induced damage, nanosized Ga-based precipitates in FCC Cu are believed to have the largest effect on the flow strength.[14] Thus, the current analysis will focus on the presence of such Ga precipitates in the damaged layer, which represents the worst case scenario. These precipitates are treated as spherical obstacles having a radius $r_p=1.4$ nm. Since these precipitates have a much smaller size compared to the volume of the simulated pillars, the strain field of these precipitates can be ignored. In addition, the precipitates are randomly distributed in the outer circumference of the simulated micropillar, with an average inter-precipitate spacing of $l_p=10.2$ nm, and within a layer of depth t from the surface of the pillar. These values are in agreement with experimental observations in Cu grains that were FIB machined.[15] The layer depth is also varied, such that $t=25$, 50, and 100 nm, respectively. These values are chosen to mimic the experimentally predicted depth, which can be in the range $10\leq t\leq100$ nm, depending on the ion energy, incident angle of the ions, and the target material.[14,18–20]

From 3D dislocation dynamics simulations performed by Takahashi and Ghoniem,[27] it was reported that the critical resolved shear stress (CRSS) required to move a straight dislocation through a one-dimensional precipitate array is mainly dependent on the size of the precipitates, interprecipitate spacing, and the ratio of the precipitate-to-matrix shear modulus. From their results, it was shown that the CRSS for spherical precipitate, having diameters in the range $2.5\leq r_p$ ≤5 nm, can reach up to $(0.3\sim0.4)\times\mu_m b/l_p$ for soft precipitates having $\mu_p/\mu_m\ll1$, and up to $(0.6\sim0.85)\times\mu_m b/l_p$ for strong precipitates having $\mu_p/\mu_m\gg1$. On the other hand, in the intermediate range where $0.1<\mu_p/\mu_m<3$, the CRSS is in the range $(0\sim0.4)\times\mu_m b/l_p$. Here, μ_p and μ_m are the shear moduli of the precipitate and matrix, respectively. In addition, the precipitate strength was shown to decrease with decreasing precipitate size. Since the size of the precipitates in our simulations are much smaller than those used in,[27] their strength would be expected to be smaller. Based on these results and due to the lack of data on the properties of
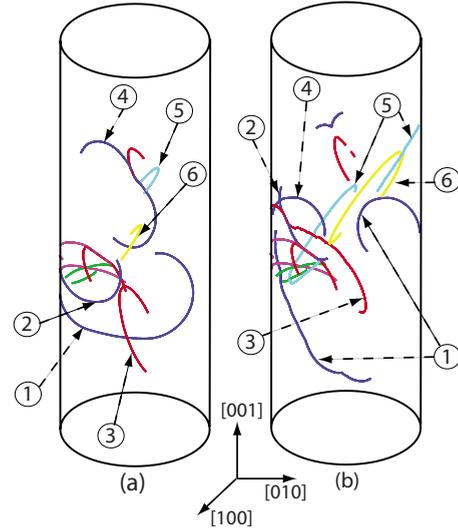

FIG. 1. (Color online) Microstructure of a $D=0.75$ μm micropillar at 0.17% strain. (a) No damage layer. (b) Damage layer depth $t=100$ nm and precipitate strength of $\sigma_p=750$ MPa is used. The precipitates are not plotted for clarity. The numbers encircled reference the same dislocations in both simulations.

the nanosized intermetallic Ga precipitates forming during FIB milling, we chose to vary the strength of the precipitates in our calculations such that their CRSS is in the range $(0.1\sim0.4)\times\mu_m b/l_p$. Thus, we vary the CRSS such that σ_p $=100$, 250, 500, and 750 MPa, respectively. When a dislocation propagates in the micropillar, and meets one of these precipitates, it will get pinned. The dislocation then will not cut through the precipitate until the local resolved shear stress equals the CRSS of the precipitate, σ_p. When this critical strength is reached, the dislocation is released and the precipitate is destroyed.

Each time a dislocation shears through a precipitate, its strength will be reduced. Takahashi and Ghoniem[27] reported that the strength of a 2.5-nm precipitate can reduce by 10% after the first two times a dislocation shears through it. Two more passes would reduce it even more by 30% of its original strength. Finally, as the precipitate is completely sheared through, the precipitate strength drops by 40–45 %. In our current simulations, since the applied load is not allowed to drop, and after the first dislocation shears through a precipitate, the local CRSS at this precipitate will not change much for subsequent dislocations arriving at the location of this precipitate. Also, since the strength of the precipitate should be reduced, the presence of an already sheared precipitate on subsequent dislocation motion will be minimal. Thus, to minimize the amount of computations, the precipitate can safely be assumed to be destroyed after the first dislocation shears through it. In other cases were the applied stress is allowed to drop, this assumption would not be valid.

Figure 1 shows the microstructure after 0.17% strain for a simulated micropillar having size $D=0.75$ μm. The initial dislocation density was $\rho=3.4\times10^{12}$ m^{-2}. Figure 1(a), illustrates the micropillar simulated without a FIB damage layer. In this case, a flow strength of 246 MPa was reached. Figure 1(b), shows the same simulated micropillar but with t
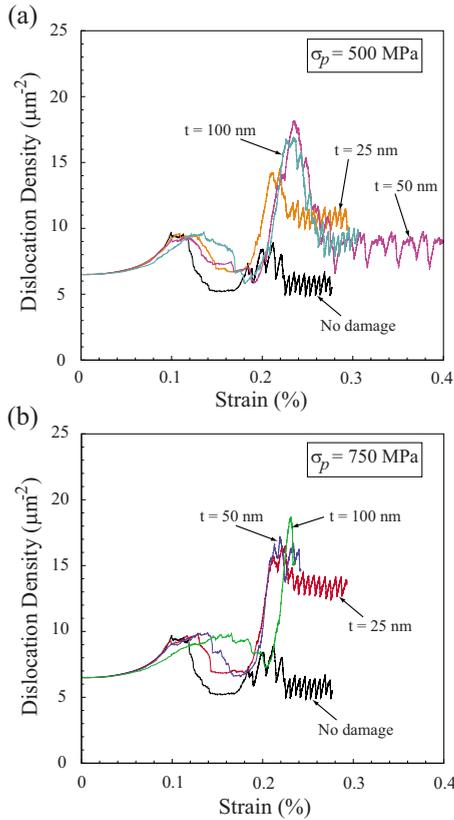
FIG. 2. (Color online) Dislocation density versus strain for a $D=0.75$ μm micropillar having two precipitate strengths: (a) $\sigma_p=500$ MPa and (b) $\sigma_p=750$ MPa. Both cases produce an initial increase in dislocation density, however this density persists into the steady-state regime for the larger precipitate strength.

$=100$ nm, and $\sigma_p=750$ MPa. A higher flow strength of 273 MPa was reached. In this case, the precipitates acted as an additional barrier to the dislocation motion near the surface, and thus a higher strength was required for the dislocation to penetrate through this damaged layer. Examples of observed microstructure changes from Fig. 1 are: (1) sources that were activated when the damage layer was not included, are trapped when including the damage layer (dislocations 2 and 3); (2) additional sources being activated, when including the damage layer, due to the higher flow strength levels (dislocation 6); (3) some dislocation locks/dipoles were prevented due to the changes in the microstructure (dislocation 4).

In Fig. 2, the dislocation density versus strain for a $D=0.75$ μm micropillar, with an initial dislocation density of $\rho=6.4\times10^{12}$ m^{-2}, is shown. Results for various damage layer depth, and $\sigma_p=500$ and 750 MPa are shown, respectively. It is observed that for $\sigma_p=750$ MPa, the dislocation density increases by a factor of ~2.5 compared to the simulation without the damage layer. The simulation results show a sharp increase, then decrease to a steady state, in the dislocation density as shown in Fig. 2. As the largest sources in the pillar are first activated, part of the dislocations will get pinned in the damage layer, while the remainder of these sources are free to expand in the precipitate-free region. If the local strength is not high enough for the dislocation to penetrate through the damage layer, a dislocation pileup
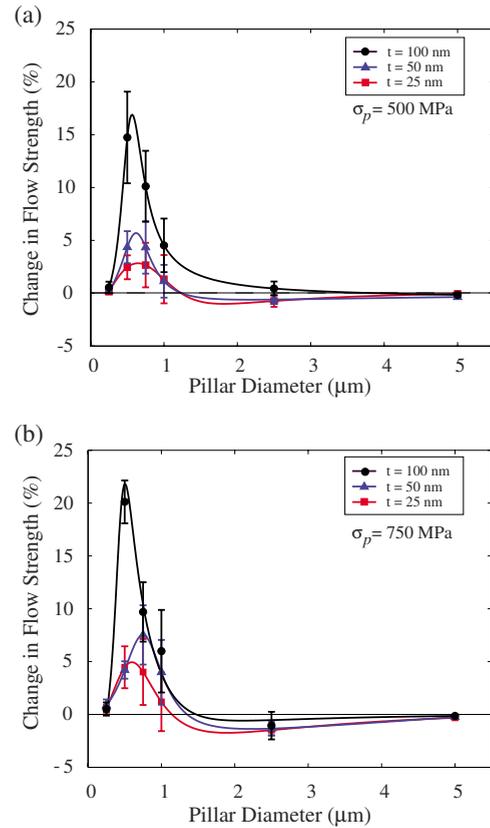

FIG. 3. (Color online) The average percentage change in the computed flow strength, for different micropillar sizes and precipitate layer depth. (a) $\sigma_p=500$ MPa; (b) $\sigma_p=750$ MPa. The error bars are the standard deviation of the simulated results from the average and the solid lines represent the best fit for each damage depth.

builds up, and the dislocation density sharply increases. After one or two passes from those activated sources, a higher local strength is reached that can destroy the precipitates and the dislocation pileups escape the pillar. Once this occurs, the dislocation density rapidly decreases to a lower steady-state value. It is also observed that some activated dislocations that would have escaped the pillar if the damage layer was removed, will instead be trapped in the pillar. The number of trapped dislocations increases as the precipitate strength increases, and a higher steady-state dislocation density is reached.

Figure 3 shows the percentage change in the computed flow strength as a function of pillar diameter, for $\sigma_p=500$ and 750 MPa, respectively. Here, the percentage change is defined as $[(\sigma_f^{(d)}-\sigma_f)/\sigma_f]\times100\%$, where $\sigma_f^{(d)}$ is the computed flow strength when including the damage layer, and σ_f is the flow strength for the same pillar and initial dislocation structure but with no damage layer. For each pillar size between 0.25 and 1.0 μm, six to eight different initial dislocation distributions with different initial dislocation densities were simulated, for each damage depth and precipitate strength. In addition, the 2.5 and 5.0 μm pillars were simulated with three and two different initial dislocation distributions and initial dislocation densities, respectively.

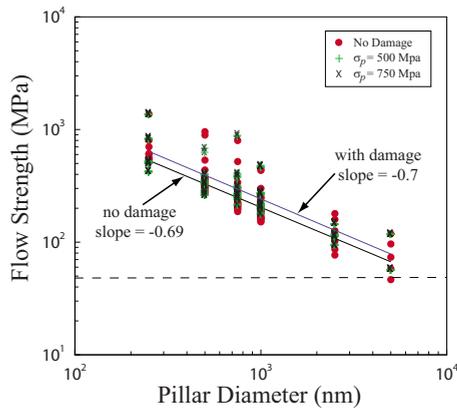It is clear from Fig. 3 that there is a window of micropillar

FIG. 4. (Color online) A comparison of the flow strength at 0.5% strain versus micropillar size, showing results from simulations with no damage layer (Ref. 25), and the current simulation results with a layer of precipitates having strength 500 and 750 MPa. Results for all three layer depths are included.

sizes for which the flow strength is dependent on the damage layer. For micropillars having sizes at and below 0.25 μm, the number of sources in the pillar are limited, and the applied strength needed to activate the dislocation sources is already high.[25] Thus, the activated dislocations can overcome the precipitates without the need for a higher strength. In addition, for pillars having diameters equal to or greater than 2.5 μm, the number of sources in the pillar is high, and the local dislocation stress field becomes strong enough, due to the initial dislocation pileup, to overcome the damage layer without the need for any additional increase in strength. On the other hand, for simulated pillars having sizes between 0.5–1.0 μm, the effect of the damage layer is observed to increase the flow strength by 2.5–23 %, depending on the depth of the damage layer, and the strength of the precipitates. For this window of simulated pillar sizes, the competition between the numbers of sources available, local dislocation stress field, strength required to activate dislocation sources, and the precipitate strength, all comes into play. Simulations with a precipitate strength of 100 and 250 MPa revealed similar observations, but the increase in the flow strength was limited to 2.5–10 % for pillar sizes between 0.5–1.0 μm. Softening was also observed in some simulated pillars having sizes 1.0 and 2.5 μm. This is because the evolving microstructure (i.e., dislocation speed and shape) changes in the presence of the damage layer, and dipoles/locks that would have formed in the absence of the damage layer, are instead avoided. Thus, a lower strength would be required to activate the dislocation system. The maximum softening observed was 2.5%.

Figure 4 shows a comparison of the computed flow strength versus micropillar size, for previous DD simulations that do not include a damage layer,[25] and the current results with different precipitate strength and damage layer depth. It is observed that even for the strongest precipitate strength and damage layer depth, the strength scaling power-law exponent is at best weakly dependent on the presence of a damage layer. Including the damage layer may alter the underlying dislocation microstructure, however, even for the strongest precipitates and deepest defect layers, this produces

less than a 25% change in the flow strength. This is an order of magnitude smaller than the effect of varying the source size distribution, which can lead to as much as 200–300 % change in the flow strength for each pillar size.

Rao *et al.*[23] showed that a higher initial dislocation density will result in a weaker scaling response and vice versa. For large pillar sizes, simulations having a higher initial dislocation density was observed to result in a higher flow stress. This is due to the dominance of forest-hardening processes for these larger pillars. Such trend is reversed at smaller sizes were higher dislocation densities will result in a weaker pillar. They also observed that the scatter is considerably less for high dislocation density simulations compared with low-density simulations. Nevertheless, the observed scatter is still an order of magnitude larger than the effect of the damage layer reported in the current study. Thus, the dependency of the flow strength on the initial dislocation density will not be affected by the presence of the damage layer.

It should be mentioned that Kiener *et al.*[4] performed some simplified estimates based on the precipitate hardening knowledge and predicted that the strength of the pillars can increase significantly over 50% for pillars smaller than 1.0 μm. This is in fact contradictory to all experimental evidence that show that for such small pillars the FIB induced damage seems to have a relatively small effect.[5,6] While such simplified estimates may provide some insight on the role of intermetallic hardening, they defiantly do not give decisive conclusions and may not be entirely correct. Such simplified estimates fail to take into account the complex 3D dislocation structures that are present in the pillar and the complex stress distribution that cannot be accounted for without full 3D dislocation dynamic simulations. The results of the current study are observed to by in general agreement with all experimental observations and provide some insight on the mechanisms involved with the deformation process.

In addition, there have been some attempts to investigate the effects of other types of radiation damage on the multiplication and motion of dislocations. Rodney and Martin[28] performed molecular-dynamics simulations to investigate the dislocation pinning by interstitial loops in nickel crystals. They concluded that the dislocation loops represent rather weak dispersed barriers and their effect on hardening was small. Another important point that needs thorough investigation is the effect of the presence of an amorphous layer. This layer can have a width in the order of tens of nanometer[29] and acts as a barrier to dislocation motion. Simplified two-dimensional DD calculations were performed to study the effect of an impenetrable layer on the motion of dislocation in Cu thin films.[30] It was shown that the flow strength increases with the presence of an impenetrable layer by about 20% for films having 1.0 μm thickness. Although more 3D DD detailed investigations need to be performed, such results would suggest that the effect of an amorphous layer would be the dominant effect at the smaller micropillar sizes.

Finally, more detailed experimental investigations are still required to completely characterize the exact microstructure forming due to the FIB milling. This would aid in building and performing full 3D DD simulations that can correctly

represent the experimental microstructure, which may result in a better understanding of the influence and the relative importance of the different FIB induced defects on the plasticity of micropillars.

In summary, the effect on plasticity of FIB induced damage during the fabrication process of micropillars was examined. A layer of nanosized precipitates was introduced into dislocation dynamic simulations to represent such FIB induced damage. The influence of the layer depth and strength of the precipitate was then analyzed. It should be noted that, the depth of the damage layer is a function of the incident angle of the ion beam, the ion acceleration energy, and the milled material. Thus, the current results should be viewed as representing a qualitative understanding of the effects of the presence of such a layer on the response of micropillars. We show that for a window of simulated micropillar sizes between 0.5 and 1.0 μm, the flow strength can increase by 10–23 % for $\sigma_p = 750$ MPa and damage depth of 100 nm. In addition, the dislocation density can increase by a factor of

$\sim$2.5. For pillars sizes that are outside this window (i.e., $D < 0.5$ μm and $D > 1.0$ μm), a negligible effect on the flow strength is observed. Finally, the current results show that the obstacles that form during the FIB milling do alter the microstructure of micropillars. However, even for the strongest obstacles and deepest defect layers, the effect is less than 25% of the flow stress expected in undamaged micropillars. Since the observed and calculated size strengthening for fcc metals is an order of magnitude larger than this, it can be concluded that such obstacles that could form in these micropillars have a relatively small effect on the observed size dependence.

---

*Also at Universal Technology Corporation, Dayton, OH 45432, USA; jaafar.el-awady@wpafb.af.mil

[1] A. Karmous, A. Cuenat, A. Ronda, I. Berbezier, S. Atha, and R. Hull, Appl. Phys. Lett. **85**, 6401 (2004).

[2] C. Nam, J. Kim, and J. Fischer, Appl. Phys. Lett. **86**, 193112 (2005).

[3] D. Dimiduk, M. Uchic, and T. Parthasarathy, Acta Mater. **53**, 4065 (2005).

[4] D. Kiener, C. Motz, T. Schöberl, M. Jenko, and G. Dehm, Adv. Eng. Mater. **8**, 1119 (2006).

[5] Julia R. Greer and William D. Nix, Phys. Rev. B **73**, 245410 (2006).

[6] Z. Shan, R. Mishra, S. Asif, O. Warren, and A. Minor, Nature Mater. **7**, 115 (2008).

[7] C. Frick, B. Clark, S. Orso, A. Schneider, and E. Arzt, Mater. Sci. Eng., A **489**, 319 (2008).

[8] Steffen Brinckmann, Ju-Young Kim, and Julia R. Greer, Phys. Rev. Lett. **100**, 155502 (2008).

[9] S. Shim, H. Bei, M. Miller, G. Pharr, and E. George, Acta Mater. **57**, 503 (2009).

[10] M. Marko, C. Hsieh, R. Schalek, J. Frank, and C. Mannella, Nat. Methods **4**, 215 (2007).

[11] Y. Chan, A. Ngan, and N. King, J. Mech. Behav. Biomed. Mater. **2**, 375 (2009).

[12] R. Wirth, Chem. Geol. **261**, 217 (2009).

[13] S. Rubanov and P. Muroe, J. Microsc. **214**, 213 (2004).

[14] D. Kiener, C. Motz, M. Rester, M. Jenko, and G. Dehm, Mater. Sci. Eng., A **459**, 262 (2007).

[15] J. Marien, J. Plitzko, K. R.-M. Spolenak, R. Keller, and J. Mayer, J. Microsc. **194**, 71 (1999).

[16] J. Yu, J. Liu, J. Zhang, and J. Wu, Mater. Lett. **60**, 206 (2006).

[17] B. Singh and S. Zinkle, J. Nucl. Mater. **206**, 212 (1993).

[18] T. Ishitani, K. Umemura, T. Ohnishi, T. Yaguchi, and T. Kamino, J. Electron Microsc. **53**, 443 (2004).

[19] J. Michael, Microsc. Microanal. **12**, 1248 (2006).

[20] K. Thompson, D. Lawrence, D. Larson, J. Olson, T. Kelly, and B. Gorman, Ultramicroscopy **107**, 131 (2007).

[21] M. Uchic, D. Dimiduk, J. Florando, and W. Nix, Science **305**, 986 (2004).

[22] M. Uchic, P. Shade, and D. Dimiduk, Annu. Rev. Mater. Res. **39**, 361 (2009).

[23] S. Rao, D. Dimiduk, T. Parthasarathy, M. Uchic, M. Tang, and C. Woodward, Acta Mater. **56**, 3245 (2008).

[24] H. Tang, K. W. Schwarz, and H. D. Espinosa, Phys. Rev. Lett. **100**, 185503 (2008).

[25] J. A. El-Awady, M. Wen, and N. M. Ghoniem, J. Mech. Phys. Solids **57**, 32 (2009).

[26] J. A. El-Awady, S. B. Biner, and N. M. Ghoniem, J. Mech. Phys. Solids **56**, 2019 (2008).

[27] A. Takahashi and N. Ghoniem, J. Mech. Phys. Solids **56**, 1534 (2008).

[28] D. Rodney and G. Martin, Phys. Rev. B **61**, 8714 (2000).

[29] J. McCaffrey, M. Phaneuf, and L. Madsen, Ultramicroscopy **87**, 97 (2001).

[30] L. Nicola, Y. Xiang, J. Vlassak, E. Van der Giessen, and A. Needleman, J. Mech. Phys. Solids **54**, 2089 (2006).